A Theoretical Study of the Lake and Land Breezes of Circular Lakes

J. NEUMANN AND Y. MAHRER[1]

Department of Atmospheric Sciences, The Hebrew University, Jerusalem, Israel

(Manuscript received 30 July 1974; in revised form 3 March 1975)

ABSTRACT

In this paper the authors study the lake and land breezes of a mesometeorological system consisting of a circular lake and a level land area surrounding it. It is assumed that initially the atmosphere is at rest, the meteorological variables being uniform along horizontal planes. At time $t=0$, a diurnal temperature wave is imposed on the land surface and the resulting circulation is studied through the application of the nonlinear equations of motion and heat conduction for an axially symmetric flow system. In the numerical solution we consider two lake sizes: one of 25 km radius ("small" lake) and the other one of 50 km radius ("large" lake).

In both lake-size cases the landward penetration of the cool lake air takes place along a front. As the lake breezes are divergent horizontally, and those of the small lake are more strongly divergent, and as horizontal divergence of winds tends to dissolve fronts, the front spearheading the breezes of the large lake is more fully developed. For the same reason, the dynamic developments along the lake-breeze front of the large lake are more intense. Thus the evolution of a pressure low, the deformation of the temperature field (and, presumably, of the water-vapor concentration field), and the circulation forming about the front of the large lake are more pronounced than is the case for the small lake. Relatedly, the velocities of the breezes of the large lake are greater than those of the small lake. This feature as well as the problem of the rate of advance of the lake-breeze front is explored on the basis of dynamical equations.

The *general* pressure field shows some unexpected developments in the afternoon hours. Because of the strong horizontal divergence of the lake breezes, the pressure falls nearly uniformly by about 1 mb over the whole of our mesometeorological system.

The land breezes are weak over the land but of some strength over the lake. Due to the horizontal convergence of these breezes, a cell of upward motion (weak) develops over the central area of the lake.

1. Introduction

In earlier papers we have studied the dynamics of sea and land-breeze circulation for straight coasts (Neumann and Mahrer, 1971 and 1973) and for circular islands (Neumann and Mahrer, 1974). In the present paper we wish to complete the study of the systems of sea and land-breeze circulations that can be treated as two-dimensional in space by investigating the lake and land-breeze circulation (LLBC) for circular lakes. As before, we will examine the full 24-hour cycle.

Observations on the LLBC of some lakes were published at least 175 years ago. In 1799 Ellicott (1799) recorded his observations concerning the lake and land breezes on the Pennsylvania coast of Lake Erie. He makes the perceptive remark (p. 224) that the "phenomena [observed by him] in all probability are common to all large lakes of fresh water."

In Europe the lake whose breezes have received a great deal of attention is Lake Constance (Kopfmueller, 1922, 1923, 1924; Peppler, 1936; Roenicke, 1967; Huss and Stranz, 1970). In the United States, Lake Michigan, and especially, the Chicago area, have been the subject of a comparatively large number of investigations, beginning with a paper by Hazen (1883), who used a lake-crib station 5 km offshore from Chicago for observing winds over the "open" lake. In more recent years several papers have dealt with theory, prediction, and air pollution problems in relation to the lake-breeze circulation of Lake Michigan by Hall, Hewson, and Moroz (east coast of Lake Michigan), Moroz, and by Lyons and his associates (Chandlik, Cole, Olsson). For detailed references to these studies, see Lyons's (1972) paper. A still more recent paper on Lake Michigan is by Lyons and Olsson (1973), who examine in some detail the characteristics of the lake and land breezes of Lake Michigan and the effects of these breezes on the transport and "recycling" of pollutants.

Additionally, but relating to another great lake, we wish to mention a study by Fraedrich (1968), who investigated the wind divergence, vertical velocities, and vorticity for the region of Lake Victoria, East Africa.

[1] Now at the Department of Environmental Science, University of Virginia, Charlottesville, Va. 22903.

As to idealized models, Fraedrich (1971, 1972) constructed an axisymmetric, linearized, steady-state model representing nocturnal conditions with Lake Victoria's case in mind. Our model, also, is axisymmetric, but it is nonlinear and time-dependent in the sense that it covers, as was pointed out above, the 24-hour diurnal cycle.

About the time that the present paper was in the draft stage, there appeared Pielke's (1974) three-dimensional model for the sea breezes (of South Florida). Being three-dimensional, his model is adaptable, in principle, to any coast configuration. There are differences between the subgrid parameterizations of his model and of the model adopted by us. An application of our model to the case of circular lakes is all the more of interest as it affords comparison with the published results of our studies for circular islands and for straight coasts. All these three cases have been investigated by us on the basis of the same subgrid parameterization.

2. The model

a. General remarks

We consider a circular lake surrounded by a flat, aerodynamically uniformly rough land surface. Since our prime interest is in circulations wholly due to differential heating, we set out from an atmosphere initially,[2] $t<0$, at rest in hydrostatic equilibrium, the meteorological variables being constant along horizontal surfaces (the earth curvature is neglected). And since we disallow large-scale pressure gradients and motions associated with them, and, further, since we do not contemplate a linear scale greater than 100–200 km for the mesometeorological system lake and environs, we can neglect the variation with latitude of the Coriolis parameter. Thus, our flow system is axially symmetric. At time $t=0$, which we take to correspond with 0800 h solar time, we impress on the land surface a diurnal temperature wave; the lake-surface temperature is taken to remain constant. Due to heating of the land, motion sets in the atmosphere, turbulence develops, and the temperature and pressure distributions change. We assume that, near the surface, turbulence is responsible for the vertical transfers of horizontal momentum and sensible heat; higher up, horizontal as well as vertical motions become important in the transfer processes. Water-vapor transport is not mentioned because the circulation is taken to be "dry," but in Section 6 consideration will be given to the plausible form of the water-vapor distribution. The possiblity of a significant horizontal diffusion of momentum and heat is discussed briefly in Section 4 of our "island paper" (Neumann and Mahrer, 1974). The conclusion of the said discussion is that the use of finite differences, even of a horizontal grid as short as 2.5 km as adopted by us, outweighs the estimated magnitude of horizontal diffusion as a result of the smoothing procedure employed in this study.

Following Estoque (1961, 1962) we divide the atmosphere affected by the LLBC into two layers: i) a relatively thin surface layer in which the vertical fluxes of momentum and heat are constant with height, and, surmounting it, ii) a transition layer in which the equations of motion proper apply. We take that the thickness of the former is 25 m and assume, as was done also in Estoque's and our earlier studies that the combined depth of the two layers is 2 km.

b. Equations of the constant-flux layer: $0\leqslant z\leqslant h$, $h=25m$

Taking the eddy viscosity equal to the eddy conductivity, we have

$$\frac{\partial}{\partial z}\left(K\frac{\partial V}{\partial z}\right)=0 \quad V=(u^2+v^2)^{\frac{1}{2}}, \quad \frac{\partial}{\partial z}\left(K\frac{\partial \theta_T}{\partial z}\right)=0, \quad (1)$$

where

$$K=\lambda z^2\left(\frac{g}{\tilde{\theta}}\left|\frac{\partial \theta_T}{\partial z}\right|\right)^{\frac{1}{2}} \qquad \text{for } \mathrm{Ri}<-0.03 \qquad (2a)$$

$$K=[k_0(z+z_0)(1+\alpha\,\mathrm{Ri})]^2\frac{\partial V}{\partial z} \qquad \text{for } |1/\alpha|>\mathrm{Ri}\geq -0.03, \qquad (2b)$$

and

$$K=2\times 10^4\ (\mathrm{cm^2\ s^{-1}}) \qquad \text{for } \mathrm{Ri}\geq |1/\alpha|. \qquad (2c)$$

We have adopted the following values: $\lambda=1$, $z_0=2$ cm for the land, and $z_0=0.5$ cm for the lake, the latter allowing for a measure of roughness of the lake surface.[3] As to α, we were forced to assign to it the value -0.03, or a value close to -0.03; a physical interpretation of the phenomenon was proffered in Section 2a of our "island study."

c. Equations of the transition layer: $h\leqslant z\leqslant H$, $H=2$ km

We place the origin of a cylindrical coordinate system at the center of our circular lake. Since we assume an axisymmetric flow, all derivatives with respect to the azimuthal angle about the z-axis vanish. Under such conditions, and using the symbol M for the magnitude of the relative momentum, the equations of motion, continuity, heat conduction, etc., are as

[2] See list of symbols in the Appendix.

[3] See Section 3b in Neumann and Mahrer (1974) where the background of this choice of λ is reviewed.

follows:

$$\frac{\partial u}{\partial t}=-u\frac{\partial u}{\partial r}-w\frac{\partial u}{\partial z}+\frac{M}{r}\left(f+\frac{M}{r^2}\right)-\frac{1}{\rho}\frac{\partial p}{\partial r}+\frac{\partial}{\partial z}\left(K\frac{\partial u}{\partial z}\right) \quad (3)$$

$$\frac{\partial M}{\partial t}=-u\frac{\partial M}{\partial r}-w\frac{\partial M}{\partial z}-fru+\frac{\partial}{\partial z}\left(K\frac{\partial M}{\partial z}\right) \quad (4)$$

$$\frac{\partial w}{\partial t}=-u\frac{\partial w}{\partial r}-w\frac{\partial w}{\partial z}-\frac{1}{\rho}\frac{\partial p_T}{\partial z}-g \quad (5)$$

$$\frac{\partial \theta}{\partial t}=-u\frac{\partial \theta}{\partial r}-w\frac{\partial \theta_T}{\partial z}+\frac{\partial}{\partial z}\left(K\frac{\partial \theta_T}{\partial z}\right) \quad (6)$$

$$\frac{\partial w}{\partial z}=-\frac{1}{r}\frac{\partial (ru)}{\partial r} \quad (7)$$

$$M=rv, \quad p_T=\rho R_0 T_T \quad \theta_T=T_T\left(\frac{p_0}{p_T}\right)^{R_0/C_p} \quad (8)$$

$$K=K(h)\frac{H-z}{H-h}. \quad (9)$$

d. Initial conditions, $t<0$

$$p_1(z=0)=1000 \text{ mb} \quad (10)$$

$$T_1(z=0)\equiv\theta_1(z=0)=27°\text{C},$$

$$T_1(z)=27-6.5\times10^{-5}z \ (z \text{ in cm}). \quad (11)$$

e. Boundary conditions, $t\geq 0$

Before listing the boundary conditions, we wish to point out that the form adopted for the diurnal temperature wave at the land surface has been influenced by Kuo's (1968, Fig. 6) paper which is based on a radiative-convective model. The present form, Eq. (14), is somewhat different from the one used earlier by us (Neumann and Mahrer, 1971; Eq. (15c)) and was adopted in numerical experimentation subsequent to our 1971 paper. As before, we let the amplitude of the first harmonic increase inland to a distance of 20 km from the coast. Beyond 20 km this amplitude is taken to be constant at its value at 20 km. The background of this decision is described on p. 535 of our 1971 study.

The boundary conditions are as follows:

$$z=0: \quad u=v=w=0 \quad (12)$$

$$T_T(r<R)\equiv T_1(r<R)=27°\text{C}, \quad T(r<R)\equiv 0 \quad (13)$$

$$T_T(R<r\leq R+20 \text{ km}, t)$$

$$=27+\left(12+\frac{x}{10}\right)\sin(15t-110)$$

$$+3.5\sin(30t+75)+0.5\sin(45t+66) \quad (14)$$

$$T_T(r>R+20 \text{ km}, t)\equiv T_T(r=R+20 \text{ km}, t) \quad (15)$$

$$T_T(r=R, t)=\tfrac{1}{2}[T_1(r<R, t)+T_T(r=R+\Delta r, t)]. \quad (16)$$

In Eq. (14), x is the landward distance from the coast in km and t is in hours with $t=0$ at midnight. The same equation implies that near the lake the land temperature amplitude is about 13°C, while further inland it amounts to about 15°C. It should be stressed that these amplitudes relate to the land surface "proper" and not to air temperatures at some standard height near the ground.

$$z=H: \quad u=v=w=\theta=p^*=0 \quad (17)$$

$$r=0: \quad u=v=0 \quad (18)$$

$$r=R+L: \quad w=p^*=0, \quad \frac{\partial}{\partial r}(ru,M,\theta)=0. \quad (19)$$

We are using a *staggered* grid (see Section 3), and this explains why w, θ, and p are not specified for $r=0$.

3. Numerical aspects

As in our previous studies, we follow a procedure proposed by Chorin (1968), which we have extended to include the Coriolis terms. As in our earlier studies (1973, 1974), we apply Liebmann's "accelerated" method to obtain the pressure by iteration from a Poisson-type equation. The essential steps of the numerical procedure are described in brief in the Appendix to the second of our aforementioned studies.

We use a staggered grid with

u,v computed at

$$r=(i-1)\Delta r, \quad i=1,\ldots,\left(\frac{R+L}{\Delta r}+1\right), \quad (20)$$

and

w,p,T,θ computed at

$$r=(i-1/2)\Delta r, \quad i=1,\ldots,\frac{R+L}{\Delta r}. \quad (21)$$

In consequence of Eqs. (20) and (21), boundary conditions at the lake center had to be imposed on u and v only. The radial distance L, counted from the coast to the inland boundary of the integration, was so chosen that $R+L$ is an integral multiple of Δr.

Our studies have been carried out with respect to two model lakes as set out in Table 1.

A study by Pielke (1972) compares a hydrostatic model with an anelastic two-dimensional, dry, shallow primitive-equation model for various horizontal grid sizes, heat inputs, and static stabilities. Pielke finds that at horizontal-to-vertical grid ratios ≤ 3, the

TABLE 1. Data for the two model lakes and for the numerical calculation.

Radius R (km)	Distance from coast to lateral boundary inland L (km)	Horizontal grid Δr (km)	Vertical grid Δz (m)	Time step of integration $t \leq \frac{(\Delta z)^2}{2K_{max}}$ (s)	Geographical latitude ϕ
Large lake: $51.25=50+\frac{1}{2}\Delta r$	58.75	2.5	100	25	30°N
Small lake: $26.25=25+\frac{1}{2}\Delta r$	58.75	2.5	100	25	30°N

hydrostatic model becomes unsatisfactory. Especially unsatisfactory is the situation in the case of unstable density stratifications. Now, in our numerical work, the grid ratio of concern is much greater than 3 (see Table 1). Yet, in the equations of motion, Subsection 2c above, we have adopted a non-hydrostatic approach in order to keep the equations in a form appropriate to small grid ratios. Such small ratios are highly desirable in investigations where the lake-breeze front is studied in greater detail and where even our relatively small horizontal grid size entails too much smoothing with respect to the intervals nesting (momentarily) the front and across which the variation of the meteorological factors is anticipated to be large.

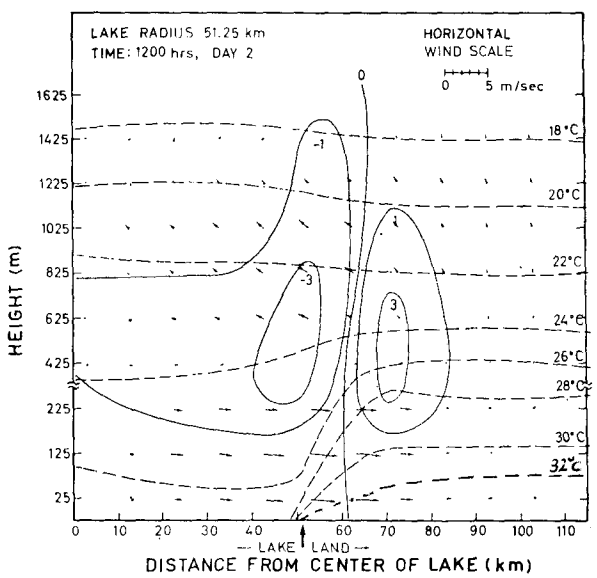

FIG. 1. Large lake (radius 51.25 km), 1200 LST. In this figure, as well as in Figs. 2, 3, 4, 5, 8, 9, 10, and 11, arrows represent the horizontal (components of) winds, with the base points of arrows placed at the pertinent altitudes. An arrow that is parallel to the abscissa and directed away from the lake conter symbolizes a wind that blows inland radially. Length of arrow indicates wind speed; see scale at right-hand-top corner of diagram. Thin, full lines are for vertical velocities (cm s^{-1}) and dashed lines for temperatures (°C). Note that the lower parts of the ordinates in all the above mentioned diagrams do not have the same height scale as their upper parts.

4. Results

The results for the large lake are the more interesting and we will turn most of our attention to them.

a. Large lake

1) HORIZONTAL WINDS AND LAKE-BREEZE FRONT (LBF)

Figures 1 through 4 show the evolution of the lake-breeze circulation from 1200 to 1500 LST (local solar time). The arrows show the horizontal components of the winds; the continuous lines depict the vertical velocities, and the dashed lines the isotherms. A comparison of these diagrams illustrates the growth and changes in all these.

As one would expect, the breezes of a lake whose shorelines are concave toward the waters are notably divergent horizontally, except within a frontal zone, the width of which diminishes as the front penetrates inland and its sharpness intensifies. The presence of horizontal convergence about the front and the intensification of the latter are evidences as to the strength of the dynamic processes taking place about the frontal "surface" which overcome the frontolytical action of

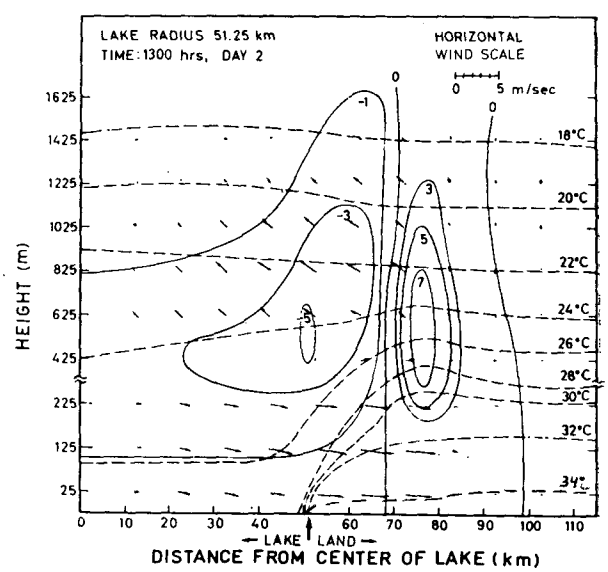

FIG. 2. Large lake, 1300 LST. Note formation of lake-breeze front at about 25 km inland from coast.

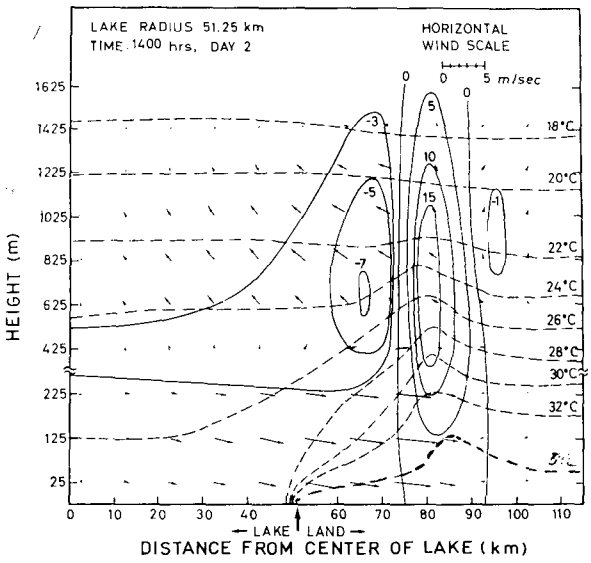

FIG. 3. Large lake, 1400 LST. Note marked uplift of isothermal surface about the front as "cold" lake air undercuts "warm" land air.

the horizontal divergence[4] "inherent" in the lake breezes of a coast that is concave toward the water body. At 1200 LST, Fig. 1, the front is about 20 km inland from the lake, the frontal convergence zone being at that time wide and weak. This lends strength to a point made recently by Clarke (1973, p. 43, footnote) which was recognized earlier by us, namely that distinct sea-breeze fronts are not observed within 10 to 20 km from the coast. At 1300 LST, Fig. 2, the front is about 25 km from the lake and the frontal convergence zone is still about 30 km wide; at 1400 LST, Fig. 3, the front is about 30 km inland but the said zone is now down to about 18 km.

The most marked development of the front is reached near 1500 LST, Fig. 4, a situation persisting close to 1600 LST (not shown diagrammatically). At these hours the circulation is so fully grown that winds astride the front are almost opposite in direction up to a height near 400 m, producing a strong horizontal convergence about the front at low altitudes and, upward motion on and just ahead of the front. The countercirculation is noted above about 600 m but the interesting point is that, from approximately 1000 m up, the winds just ahead of the front blow landward—that is, the conventional picture of countercirculation does not hold for this sector. The deviation in wind direction produces a large horizontal divergence which, in turn, contributes to the formation of a system of low pressure about the front near the surface; see Subsection 4 below and Fig. 7. We observe in the latter that this pressure low deepens as it is displaced landward with time in the afternoon up to a point when sensible heat transfer from the land is no longer capable of supplying energy for the circulation, and, as a result, the circulation begins to decay.

Lakeward, beginning from a short distance behind the front, the lake breezes are divergent, as one would expect for a coast concave toward the water body. In Subsection 5 below we will point out that it is this low-altitude divergence which brings about a *general* pressure fall, of about 1 mb, over most of our mesometeorological system (see Fig. 7), especially about and between the hours 1600 to 1800 inclusive. This general pressure fall is distinct from the localized pressure fall about the LBF.

Because a horizontally divergent flow acts frontolytically (e.g., Haltiner and Martin, 1957; p. 293) and because the lake breezes are divergent, except for the vicinity of the front, the LBF's of lakes are less well-developed than in the case of straight coastlines (Neumann and Mahrer, 1973) and still less so than is the case of circular islands (Neumann and Mahrer, 1974) where the sea breezes are highly convergent. Our *theoretical* calculations indicate that, on and near the front, the convergence/divergence amounts, order-of-magnitudewise, to 10^{-4} s^{-1}, whereas at some distance from the front, to 10^{-5}, or less. Fraedrich's (1968) figures for Lake Victoria, based on *observed* winds, are of the order of 10^{-5} s^{-1}. Lyons and Olsson (1973), using the continuity equation, compute a case (see p. 396 of their paper) where the horizontal convergence at the "wind-shift line" (~lake-breeze front) inland from Lake Michigan amounted to as much as -2×10^{-3} s^{-1}.

Figure 5 shows the circulation conditions for the *small* lake at 1500 LST, that is, for the same hour

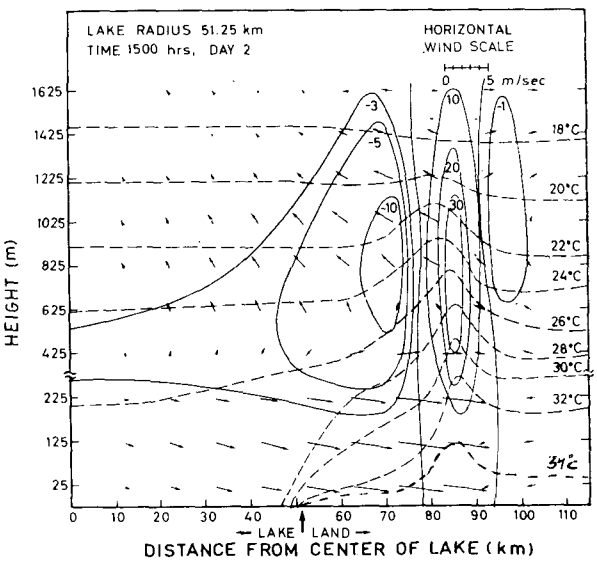

FIG. 4. Large lake, 1500 LST. Lake-breeze front near its maximum development. Winds ahead of front are nearly opposite in direction to lake breezes. Compare with Fig. 5 for small lake: the lake-breezes and front of large lake are more fully grown.

[4] For a discussion of the frontolytical effects of horizontal divergence of winds, see, e.g., Haltiner and Martin (1957), p. 293.

as Fig. 4 which relates to the *large* lake. A comparison of the two indicates that the LBF of the large lake is much better developed than that of the small lake. This is not *simply* due to the difference in size. On the contrary. Our island study (1974; see also Section 5 below) shows that several features of the sea-breeze circulation for "small" (circular) islands are more fully grown than in the case of the "large" island, the island radii being, respectively, equal to the lake radii of the present paper. In all probability, the disparities in the degree of development of the fronts for the two lake sizes are due, at about the same land-water temperature differences, to differences in the intensities of the processes of divergence/convergence. The horizontal divergence is less in the case of the breezes of the large lake than is true for the small lake and, therefore, frontolytical effects are feebler for the former. The reverse is true for the relative magnitudes and frontogenetical effects of horizontal convergence for the above mentioned two island sizes.

As is seen from Figs. 1 through 4, the rate of advance of the LBF, between 1200 and 1500 LST, is approximately 5 km h^{-1}, which is about one half the speed of the lake breeze. This estimate can be improved by extending an argument due to Prandtl (1952, p. 369), based on earlier work by von Kármán (1940). Let C denote the radial speed of the lake breezes ($\sim$cold air), F and W, respectively, that of the LBF and of the warm air ahead of the front. Then, the requirement that the dynamic pressure must be the same on both sides of the frontal surface is stated by the equation

$$\tfrac{1}{2}\rho_C(C-F)^2=\tfrac{1}{2}\rho_W(F-W)^2, \tag{22}$$

ρ_C and ρ_W being the densities of the cold and warm air, in that order. Neglecting the usually small difference between the latter two, we have that

$$F=\frac{C+W}{2}. \tag{22a}$$

A reference to Figs. 1 through 4 indicates that from 1200 to 1500 LST, C increases from about 2.5 m s^{-1} to about 4.5 m s^{-1}, whereas W changes from approximately 1 to -1 m s^{-1}, leading to a value circa 3.5 m s^{-1} for the algebraic sum of C and W, or F about 6 km h^{-1}, in fair agreement with the earlier mentioned estimate. The near-constancy of the rate of progression of the front between the above hours results from the following dynamic developments: About midday, the lake breezes are weak and the circulation about the front is but incompletely developed; the winds ahead of the front "blow" inland. Subsequently, the circulation intensifies: the lake breezes take on speed and the winds ahead of the front reverse their direction, that is, W becomes negative. The negative values

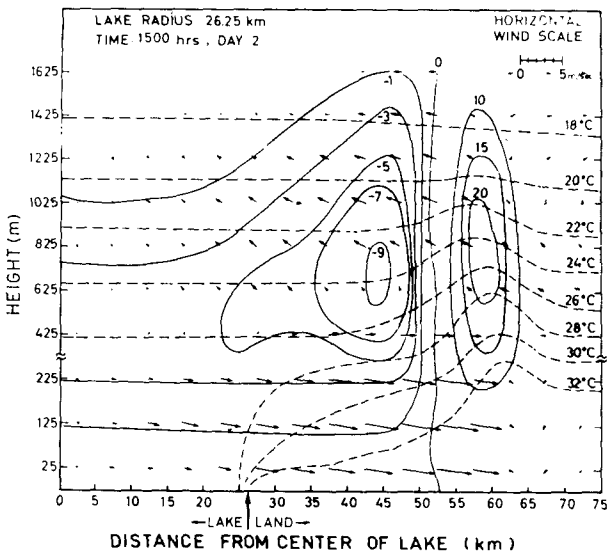

FIG. 5. Small lake (radius 26.25 km), 1500 LST. Compare with Fig. 4.

of the latter counteract the enhanced positive values of C so that F remains nearly unchanged between the hours of concern.

Data on the speed of progression of the lake-breeze front can be found, e.g., in the paper by Lyons and Olsson (1973) repeatedly referred to in the present study; some of the same data also appear in Lyons and Olsson (1972). In Fig. 8 of the 1973 paper by Lyons and Olsson, hourly positions of the lake-breeze front are plotted for the nine hours between 09 and 18 CST for the Greater Chicago Area of Lake Michigan. On 12 August 1967, the average rate of advance of the lake-breeze front is about 5.5 km h^{-1} (see their Fig. 16), while the speed of the breezes just behind the front is 2–3 m s^{-1}, that is, between about 7 and 11 km h^{-1}, or the speed of progression of the front is close to one half the speed of the breezes. On 13 August 1967, the front speed is somewhat less. It is about 4.5 km h^{-1} (see their Fig. 16), while the speed of the breezes just behind the front is 1–3 m s^{-1}, or about 4 to 11 km h^{-1}. Thus the observational data are in rather good agreement with our theoretical predictions.

Returning to the matter of countercirculation aloft, the recent paper by Lyons and Olsson (1973) contains a number of items of evidence corroborating the existence of that countercirculation in nature. One of the striking instances is a photograph (their Fig. 3) showing smoke from a power plant 30 km south of Milwaukee, Wis., during a shallow lake breeze. The plant has four stacks varying in height from 75 to 170 m above lake. Smoke from the lower stacks moves *inland* carried by the lake breeze while that from the higher stacks manages to penetrate into the *return flow* aloft.

It will be recalled (see Subsection 2b) that in our calculations we assume for the land surface a rough-

ness parameter $z_0=2$ cm. At the suggestion of a referee we have carried out a second set of calculations involving a larger roughness parameter, namely 5 cm. The results indicate an increase in the velocity of the lake breezes for the hours of an unstable thermal stratification, that is, for the hours when the breezes are at their strongest. The horizontal velocities over the land work out about 20–25% stronger than was the case for the lesser land roughness, and there is a small increase in the vertical velocities as well.

A detailed analysis of the computational results explains the intensification of the breezes as due to an enhanced land-lake temperature difference aloft, "aloft" here meaning heights from a small distance above the surface up to a few hundred meters. As one would anticipate, the assumed greater surface roughness increases the vertical turbulent transfer of heat from the ground. Turbulent transfer and vertical convection now carry a larger amount of heat upward with the consequence that the air over the rough land is warmer up to a few hundred meters than in the case of the smaller roughness—that is, the land-lake temperature difference is intensified around midday leading to a strengthening of the computed breezes.

The velocities of the breezes are little affected outside the hours of static instability.

2) Vertical velocities

Upward velocities are largest at the front where they reach 30 cm s^{-1}, Fig. 4. Since all computed variables are *averages* for a 2.5 km horizontal grid, it is almost certain that in a smaller grid net we would find larger values in the space "element" hosting (part of) the front. Lyons and Olsson (1973, p. 396) find, by calculation, that in the case of the strong horizontal convergence mentioned in Subsection 1 above, the computed upward velocity on the LBF amounted to as much as 130 cm s^{-1}.

Behind the front we have a cell of downward velocities "covering" a relatively large cross section; in the case of the large lake an additional small cell of weak downward velocities develops ahead of the front. A note confirming the existence of descending currents over the sea behind a sea breeze reaching a coastal station was published by Batty (1921). A Cosmos 144 satellite photograph, in a paper by Bugaev (1973), shows a cloud-free strip of sea coast in the rear of a sea breeze. Lyons and Olsson (1973, pp. 396–397) report large values of downward velocities behind the front over the lake as computed by them and point out, in support, that the behavior of tetroon suggests that the feature is real. They add: "Also the extremely rapid dissipation of the cumulus cloud over the lake at 1030 CST tends to confirm this particular feature in a qualitative sense, although the absolute value of the subsidence might well be questioned."

The effect of the vertical velocities on the temperature and water-vapor fields will be mentioned, respectively, in Subsection 3 below and in Section 6.

In the case of islands, the SBF (sea-breeze front) is so much sharper that the maximum upward velocity is about 50 cm s^{-1} for a "large" island (radius = 50 km), and as much as 150 cm s^{-1} for a "small" island (radius = 25 km), see Neumann and Mahrer (1974).

3) Temperatures

Before the onset of heating, the isothermal surfaces[5] were horizontal. We note in Figs. 1 through 3 how they lift up gradually in the frontal zone. Particularly strong is that upwarping at 1500 LST, Fig. 4, when the LBF is near its maximum development. Intensified turbulence and large vertical velocities of convection, associated with superadiabatic lapse rates of the early afternoon hours, have carried up a considerable amount of heat to higher strata; this transport is reflected by the uplift of the isotherms close to the front. Behind the front the isotherms drop sharply (~cool air) until they level off more or less over the lake. The peaked form of the isotherms about the front is sharpest at the lower levels, 200–300 m, where the winds are intensely convergent. The peaks broaden out higher up where horizontal divergence takes over, the divergence tending to reduce contrasts.

For what will be said below regarding the probable form of the water-vapor field, it is important to notice that the line that would connect the peaks of isotherms would slope toward the lake with height. This is a consequence of the opposite directions of winds at, respectively, low and high altitudes. At low levels, the strong lake breezes push the peaks landward; at high levels, though the winds are weaker, they carry them lakeward. The shapes of the isotherms about the front and the "backward" slope of the peaks of the same are in an approximate, rough agreement with Fig. 5.37 in Prandtl (1952, p. 370) and, in particular, with Simpson's (1969, Fig. 1) work; see, also, an earlier paper by Simpson (1964, Fig. 4). In making the comparisons, we must bear in mind the fact that the vertical scale of our diagrams is considerably expanded relative to the horizontal scale.

The same phenomenon, on a much smaller scale, is observed behind the front, underneath the cell of downward velocities. As we move lakeward from the front, we note that at distances 10–20 km there are slight downward identations in the isotherms being the effect of downward motion.

Figure 6 shows an example for the vertical profiles of temperature. The slight bulge in the line for 1400 LST, between heights of 100 to 300 m, is connected with the passage one hour earlier of the LBF.

[5] For brevity we will use from now on the term "isotherms" in place of "isothermal surfaces," all the more appropriate since in our diagrams we are looking at vertical cross sections (through the center of an axially symmetric flow).

4) Evolution of a pressure depression along the front

Our computations for all the three coast configurations show that as the SBF, or the LBF, penetrates inland an instability develops along the front. This instability is demonstrated by the evolution of a shallow, warm pressure low and an associated circulation system about the front. The energy for the growth of the circulation is supplied by sensible heat transfer from the land surface. When in the course of the afternoon the heat supply diminishes, the low fills up gradually.

The lowest value of the pressure depression about the front, 997.5 mb (Fig. 7), is reached about 1500 LST at a distance of close to 35 km inland from the coast. However, as a *general* pressure fall takes place in the system (see next subsection and Fig. 7), amounting to approximately 0.5 mb at the time, the relative low about the front is but 2 mb deep.

An application of the pressure-tendency equation, in a form appropriate to our axisymmetric flow, namely,

$$\frac{\partial p}{\partial t} = -g\int_0^H \left[\frac{1}{r}\frac{\partial(\rho u r)}{\partial r} + \frac{\partial(\rho w)}{\partial z}\right] dz, \qquad (23)$$

indicates that most of the contribution to the pressure drop about the front is due to the comparatively thick layer of horizontal divergence just above, and slightly ahead of, the front.

In the case of circular islands, where the aforementioned "high-level" divergence is particularly strong, the lowest relative pressure reached about the front is 3.1 mb; in the case of a straight coastline 2.5 mb. In the case of our "large" lake, the front is less well developed and the drop amounts to 2 mb only. It will be pointed out below that in the case of our "small" lake, the relative deepening is but 1.7 mb.

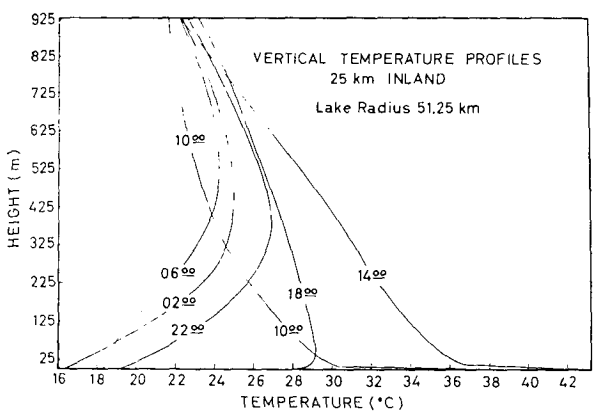

FIG. 6. Large lake: vertical profiles of air temperature at a distance of 25 km inland from coast. Note slight bulge in curve for 1400 LST, between altitudes of 100 to 300 m, a consequence of passage of the lake-breeze front one hour earlier.

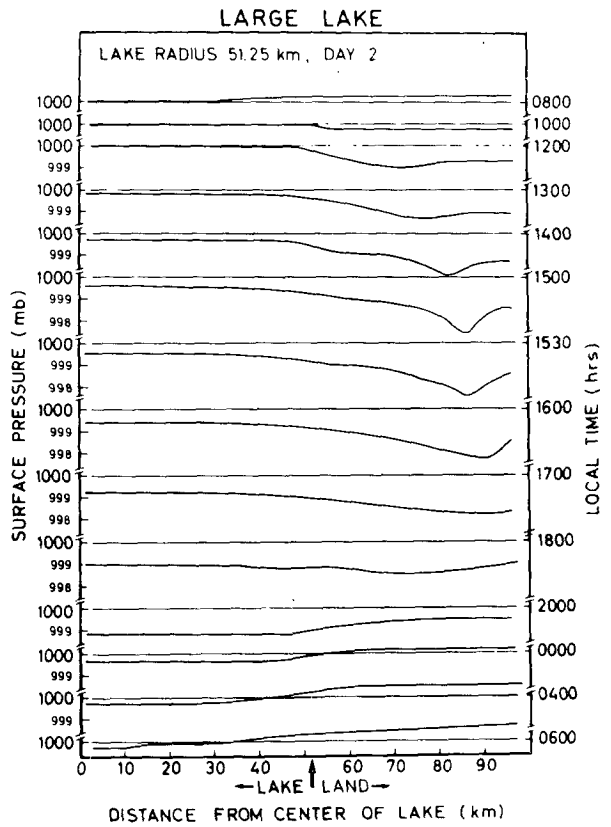

FIG. 7. Large lake: surface pressure as a function of distance from lake center and time of day. Note: development and subsequently, filling up of a shallow depression about front (compare with Figs. 1 through 4) and the *general* pressure fall late in the afternoon over the whole circulation system due to horizontal divergence of lake breezes.

5) General pressure fall in the afternoon hours

We have expected that the lake breezes should be horizontally divergent, except in the vicinity of the LBF, but the magnitude of that divergence and, particularly, its effect on the mass (~pressure) in the system, came as a surprise. Figure 7 shows that the maximum "evacuation" of mass occurs between about 1600 and 1800 LST and amounts to about 1 mb. By that time, the LBF has disappeared, or nearly so. Application of the integral in Eq. (23) demonstrates that most of that mass loss is due to the horizontal divergence of the *low-altitude* winds, that is, the lake breezes, in contrast to the frontal pressure low of the afternoon hours, which is due mainly to "high-altitude" (1 km and above) horizontal divergence. Figure 8 illustrates the marked horizontal divergence of the lake breezes.

Following up a reviewer's suggestion, we have carried out numerical evaluations of the term $(\partial p/\partial t)$ under hydrostatic conditions from the pressure tendency equation (23), by integrating it with respect to r.

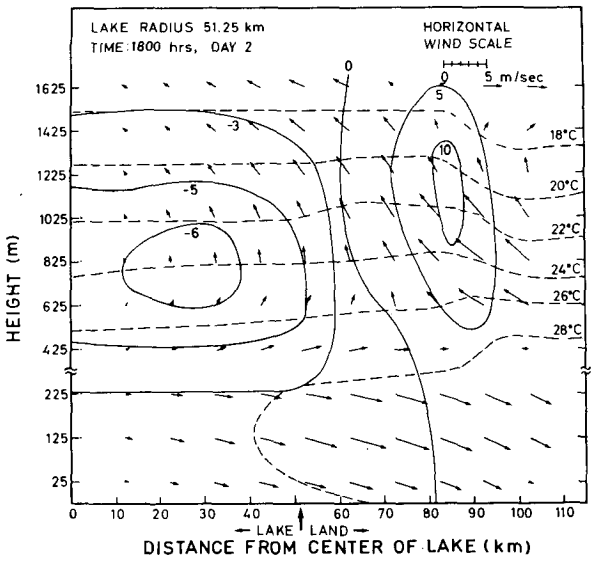

FIG. 8. Large lake, 1800 LST. Note the marked horizontal divergence of the lake breezes in the lower 250 m or so. The general pressure fall (Fig. 7) over the mesometeorological system lake and environs is due to that divergence.

Taking note of the boundary conditions on w at $z=0$ and $z=H$, we have

$$\frac{\partial \bar{p}}{\partial t} = -g\int_0^H \int_0^r \frac{1}{r}\frac{\partial}{\partial r}(\rho ru)dr\,dz. \qquad (23a)$$

For the hours between 1600 and 1800, the agreement between the values of $(\partial\bar{p}/\partial t)$ estimated from the pressure-change calculations presented above and the value obtained from the integral on the right side of (23a) is very close: -0.66 mb m s^{-1} from the former, and -0.63 mb m s^{-1} from the latter. In comparing the two sets of calculations we must, of course, remember that our model is non-hydrostatic, whereas (23) involves the hydrostatic approximation. Nevertheless, the closeness of the two foregoing results probably justifies the view that, essentially, we are dealing here with a true mass loss. Such a loss would in any case be anticipated in the case of a strongly divergent lake-breeze system, as is found in the afternoon hours in situations of a coast concave toward the water body.

At night, the pressure distribution returns to "normal" (Fig. 7). Pressure is just slightly over 1000 mb over the cool land surface, and slightly below it over the warm waters of the lake.

6) LAND BREEZES: FIGS. 9–11

The land breezes over the land, where the static stability of the air (note the temperature inversion over the land in Figs. 9 through 11) inhibits the downward flux of momentum, are weak. The land breezes are stronger over the lake, where they reach about 2.5 m s^{-1} at low altitudes. A conspicuous feature is the horizontal convergence of these breezes over the lake and the associated upward motion about the lake center. Flohn and Fraedrich (1966) attribute the observed maximum of rainfall about the center of Lake Victoria (island stations) at night to the convergence of the land breezes. Huss and Stranz (1970, p. 351) report the occasional development of clouds, even cumulonimbus, along the convergence line of the land breezes over Lake Constance. For the convergence of these breezes, see their Fig. 13.

The relative strength of our computed land breezes over the lake, large and small, reminds one of a suggestion made by Zimmern (1931, p. 39). This British scholar states that the ancient Greeks did not like, as a rule, being aboard ship at night. Nevertheless, they would sail out to sea after sunset to take advantage of the land breezes. Zimmern cites a few references to the classical Greek literature. An additional case is quoted by Neumann (1973, p. 7).

b. Small lake

The strong horizontal divergence of the lake breezes prevents the LBF from growing as fully as is the case for the large lake. Consequently, the uplift of the isotherms is less; the maximum of upward velocities are but 20 cm s^{-1} (Fig. 5) compared with 30 cm s^{-1} in the case of the large lake (Fig. 4). The relative pressure low about the front is 1.7 mb, but the general mass loss in the afternoon hours is about as great as in the case of the large lake. On the other hand, the horizontal convergence of the land breezes over the

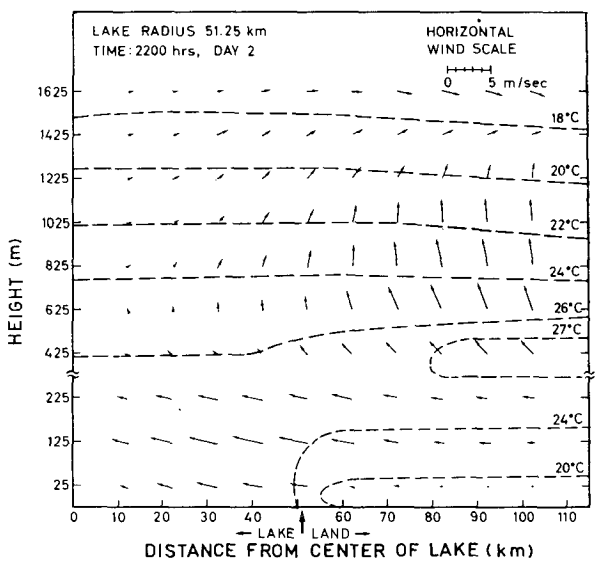

FIG. 9. Large lake, 2200 LST. Note the development of the land breezes. They are stronger over the lake than over the land. Note inversion over the land.

small lake is greater, resulting in a stronger upward motion about the lake center compared with the large lake: 6 cm s^{-1} vs 3 cm s^{-1}, respectively, in Figs. 10 and 11.

5. Large lake vs small lake: velocities of the breezes

We have noted above the much more pronounced development of the LBF in the case of our large lake. There is, however, one more feature worth commenting on. A comparison of Fig. 4 with Fig. 5 shows that the speed of the lake breezes is notably greater for the large lake. For the latter, the low-level breezes just behind the front reach 6 m s^{-1}; the parallel winds of the small lake are 4 m s^{-1}. Not unexpectedly, the opposite was found to be true for (circular) islands: our islands study indicates that the sea breezes of the "small" island are the stronger.

We do not have a full quantitative explanation for the above phenomena. It is our conjecture that the matter may be due to the greater horizontal temperature gradient produced by the dynamic development along the more intense LBF of the large lake compared with that of the small lake. The following simple analysis is a pointer toward the possible correctness of our interpretation.

Let us denote the Cartesian components of the geostrophic wind by u_g and v_g. Their equations can be put in the forms

$$\frac{f}{R_0}\frac{u_g}{T}=-\frac{1}{p}\frac{\partial p}{\partial y} \tag{24a}$$

$$\frac{f}{R_0}\frac{v_g}{T}=\frac{1}{p}\frac{\partial p}{\partial x}, \tag{24b}$$

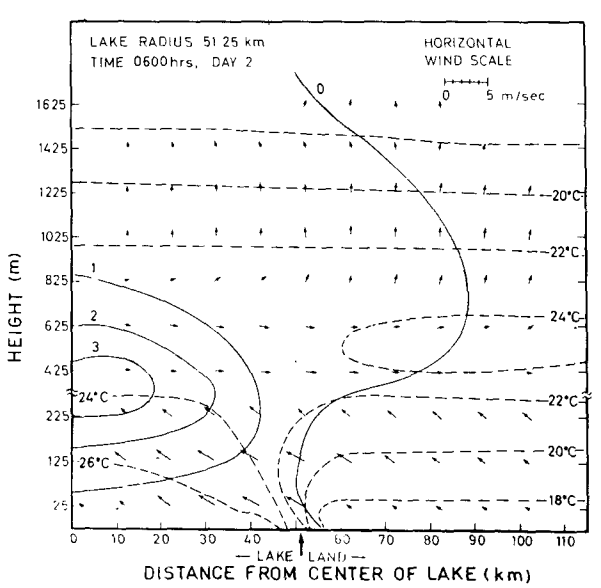

FIG. 10. Large lake, 0600 LST. Horizontal convergence of land breezes produces some vertical circulation.

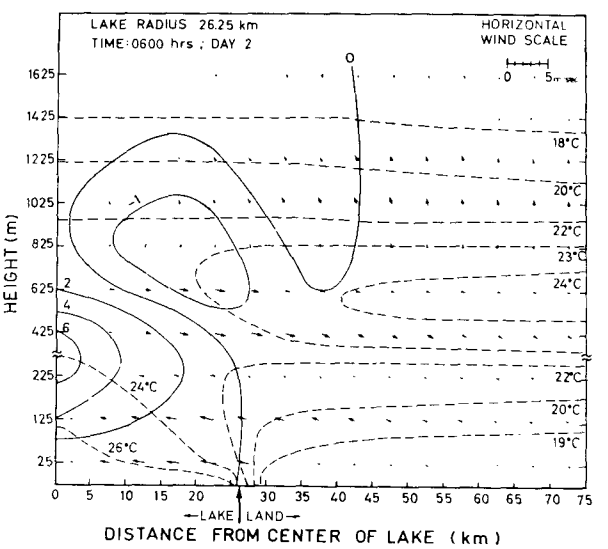

FIG. 11. Small lake, 0600 LST. Compare with Fig. 10. Horizontal convergence of the land breezes of the small lake produces a vertical circulation that is stronger than in the case of the large lake.

R_0 being the gas constant for air. Take the derivative of (24a) with respect to x and that of (24b) with respect of y, neglecting the variation of the Coriolis parameter with distance (we are not concerned here with distances greater than about 100 km). On adding the two and rearranging, we have that

$$\frac{\partial u_g}{\partial x}+\frac{\partial v_g}{\partial y}=\frac{1}{T}\left(u_g\frac{\partial T}{\partial x}+v_g\frac{\partial T}{\partial y}\right)=\frac{1}{T}\mathbf{V}_g\cdot\nabla_H T, \tag{25}$$

$\mathbf{V}_g$ being the geostrophic wind vector and ∇_H the horizontal del operator. Equation (25) means that the horizontal divergence of the geostrophic wind equals the "fractional" advection of temperature.

For the purposes of a first estimate we will take $(\partial T/\partial y)=0$ and $|\partial v_g/\partial y|$ small relative to $|\partial u_g/\partial x|$. Then,

$$\frac{1}{u_g}\frac{\partial u_g}{\partial x}=\frac{1}{T}\frac{\partial T}{\partial x}. \tag{26}$$

Equation (26) indicates that, for $u_g>0$, u_g increases in the direction of the higher temperatures (in our coordinate system, x is directed from the low surface temperatures of the lake to the high surface temperatures of the land). Since, in the case of a strongly developed front (the case of our large lake), $(\partial T/\partial x)$ will be large and positive, so will be the left side of (26): that is, we expect u_g to increase more strongly than in the instance of a comparatively small horizontal temperature gradient such as found in the case of the small lake.

6. Presumed from the water-vapor field

A LLBC study, involving the distribution of water vapor as well, would have to take account of evaporation from the lake (and from the land, if significant), just as we took note of sensible heat transfer from the land. An *incomplete* treatment of the water vapor field is found in a recent paper by Clarke (1973), and as Clarke emphasizes himself, the results are unsatisfactory.

We can make some qualitative predictions concerning the water-vapor field. Since in the LLBC dynamic developments over the lake are rather small (if we bar processes of release of latent heat) compared with what develops over the land, we can expect that, over the lake surface, the lines of equal water-vapor concentration will be mostly horizontal, just as is the case with the isothermal surfaces. Major deformations of the vapor field can be anticipated near the coast and, particularly, about the LBF. It is about the front that we have the largest vertical velocities (Fig. 4) and these, along with the enhanced turbulence close to the front, will deform the isopleths.

In Section 4a3 we have pointed out that, due to differential wind directions, the line connecting the peaks of the uplifted isotherms slopes lakeward with altitude, and that in the rear of the front, underneath the cell of downward motions, the line connecting the points of maximum "indentation" likewise trails with height. It is plausible that the water-vapor field has an essentially similar variation: just along the front moist lake air is lifted up, whereas behind the front dry air is brought down from aloft. The largest water-vapor concentration gradients should, therefore, be located across the front, especially at some height above the surface, for it is at a distance above the surface that the vertical velocities attain substantial values.

The above qualitative predictions are well supported by measurements of water-vapor concentration (pressure) across *sea* breezes by Craig *et al.* (1945) near and on the coast of Massachusetts Bay, and also, to some extent, by the data for the Madras area, India, analyzed by Hatcher and Sawyer (1947).

APPENDIX

List of Symbols

C_p	specific heat at constant pressure
f	Coriolis parameter
g	acceleration of gravity
h	thickness (25 m) of constant flux layer
H	height (2 km) of layer affected by the LLBC
k_0	von Kármán constant
K	(vertical) eddy viscosity or conductivity
L	radial distance from coast to the outer lateral boundary of the grid
M	relative angular momentum ($=rv$)
p	pressure; p_0 = reference pressure
$\bar{p}$	radially averaged pressure
p^*	deviation of pressure from its instantaneous hydrostatic value p_H: $p_T = p_H + p^*$
r	radial distance
R	radius of lake
R_0	gas constant
Ri	Richardson number
t	time
u, v, w	radial, tangential, and vertical components of velocity
V	$(u^2+v^2)^{\frac{1}{2}}$
u_g, v_g	Cartesian components of the geostrophic wind
x	distance from lake shore landward along r
z_0	roughness parameter
α	nondimensional constant (see (2b) and (2c)); $(-1/\alpha)$ is, roughly speaking, a critical Richardson number
θ	potential temperature; $\tilde{\theta}$, average potential temperature for a layer
λ	nondimensional constant (see (2a))
ρ	density ($\rho \equiv \rho_T$)
ϕ	geographical latitude

p, T, and θ without the subscripts 1 or T denote disturbance variables; subscript 1 symbolizes initial, undisturbed, value; subscript T (= total) denotes sum of initial and disturbed value, e.g., $p_T = p_1 + p$.

REFERENCES

Batty, R. P., 1921: Descending currents associated with sea breezes. *Meteor. Mag.*, **56**, 187.

Bugaev, V. A., 1973: Dynamic climatology in the light of satellite information. *Bull. Amer. Meteor. Soc.*, **54**, 394–418.

Chorin, A., 1968: Numerical solution of the Navier-Stokes equations. *Math. Comput.*, **22**, 745–762.

Clarke, R. H., 1973: A numerical model of the sea breeze (energy and mass flux across a long straight coastline due to the sea-breeze mechanism). *1st Australasian Conf. Heat and Mass Transfer*. Monash University, Melbourne, May 1973, Section I, 41–48.

Craig, R. A., I. Katz, and P. J. Harney, 1945: Sea breeze cross-sections from psychrometric measurements. *Bull. Amer. Meteor. Soc.*, **26**, 405–410.

Ellicott, A., 1799: Miscellaneous observations relative to the Western Parts of Pennsylvania, particularly those in the neighbourhood of Lake Erie. *Amer. Philos. Soc. Trans.*, **4**, 224–229.

Estoque, M. A., 1961: A theoretical investigation of the sea breeze. *Quart. J. Roy. Meteor. Soc.*, **87**, 136–146.

——, 1962: The sea breeze as function of the prevailing synoptic situation. *J. Atmos. Sci.*, **19**, 244–250.

Flohn, H., and K. Fraedrich, 1966: Tagesperiodische Zirkulation und Niederschlagsverteilung am Victoria-See (Ostafrika). *Meteor. Rdsch.*, **19**, 157–165.

Fraedrich, K., 1968: Das Land- und Seewindsystem des Victoria-Sees nach aerologischen Daten. *Arch. Meteor. Geophys. Biokl. A.*, **17**, 186–206.

——, 1971: Modell einer lokalen atmosphaerischen Zirkulation mit Anwendung auf dem Victoria-See. *Beitr. Phys. Atmos.*, **44**, 95–114.

——, 1972: A simple climatological model of the dynamics and energetics of the nocturnal circulation at Lake Victoria. *Quart. J. Roy. Meteor. Soc.*, **98**, 322–335.

Haltiner, G. J., and F. L. Martin, 1957: *Dynamical and Physical Meteorology*. New York, McGraw-Hill, 470 pp.

Hatcher, R. W., and J. S. Sawyer, 1947: Sea breeze structure with particular reference to temperature and water vapor gradients and associated radio ducts. *Quart. J. Roy. Meteor. Soc.*, **73**, 391–406.

Hazen, H. A., 1883: Report on wind velocities at the lake crib and at Chicago. *U. S. Signal Service Notes*, No. 6. Washington, Office of the Chief Signal Officer, 20+1 pp.

Huss, E., and D. Stranz, 1970: Die Windverhaeltnisse am Bodensee. *Pure Appl. Geophys.*, **81**, 323–356.

Kopfmueller, A., 1922: Der Land- und Seewind am Bodensee. *Das Wetter*, **39**, 97–107.

——, 1923: Der Land- und Seewind am Bodensee. *Das Wetter*, **40**, 33–41, 65–78, 108–115.

——, 1924: Der Land- und Seewind am Bodensee. *Das Wetter*, **41**, 1–8, 33–42.

Kuo, H. L., 1968: The thermal interaction between the atmosphere and the earth and propagation of diurnal temperature waves. *J. Atmos. Sci.*, **25**, 682–706.

Lyons, A. W., 1972: The climatology and prediction of the Chicago lake breeze. *J. Appl. Meteor.*, **11**, 1259–1270.

——, and E. L. Olsson, 1972: Mesoscale air pollution transport in the Chicago lake breeze. *J. Air Poll. Control Assoc.*, **22**, 876–881.

——, and ——, 1973: Detailed mesometeorological studies of air pollution dispersion in the Chicago lake breeze. *Mon. Wea. Rev.*, **101**, 387–403.

Neumann, J., 1973: The sea and land breezes in the classical Greek literature. *Bull. Amer. Meteor. Soc.*, **54**, 5–8.

——, and Y. Mahrer, 1971: A theoretical study of the sea and breeze circulation. *J. Atmos. Sci.*, **28**, 534–542.

——, and ——, 1973: Evolution of a sea breeze front: A numerical study. In *Climatological Research, The Hermann Flohn 60th Anniversary Volume*, Bonner Meteorologische Abhandlungen, **17**, 481–492.

——, and ——, 1974: A theoretical study of the sea and land breezes of circular islands. *J. Atmos. Sci.*, **31**, 2027–2039.

Peppler, W., 1936: Ueber die Windverhaeltnisse in der untersten Luftschicht ueber dem Bodensee und dem Ufer bei Friedrichshafen. *Beitr. Phys. Freien Atmos.*, **23**, 289–309.

Pielke, R. A., 1972: Comparison of a hydrostatic and an anelastic dry primitive equation model. NOAA Tech. Memo. ERL OD-13, Boulder, Colo., 47 pp.

——, 1974: A three-dimensional numerical model of the sea breezes over South Florida. *Mon. Wea. Rev.*, **102**, 115–139.

Prandtl, L., 1952: *Essentials of Fluid Dynamics*. London and Glasgow, Blackie & Son, 452 pp.

Roenicke, G., 1967: Untersuchungen der vertikalen Windstruktur des Land-See-Windsystems am Bodensee. *Arch. Hyg. Bakt.*, **151**, 220–231.

Simpson, J. E., 1964: Sea-breeze fronts in Hampshire. *Weather*, **19**, 208–220.

——, 1969: A comparison between laboratory and atmospheric density currents. *Quart. J. Roy. Meteor. Soc.*, **95**, 758–765.

von Kármán, T., 1940: The engineer grapples with nonlinear problems. *Bull. Amer. Math. Soc.*, **46**, 615–683.

Zimmern, A., 1931: *The Greek Commonwealth* (5th ed., revised). Oxford, Clarendon Press, 471 pp.